Systematics of equilibrium charge distributions of ions passing through a carbon foil over the ranges $Z=4-92$ and $E=0.02-6$ MeV/u

Kunihiro Shima, Noriyoshi Kuno, and Mikio Yamanouchi
Tandem Accelerator Center, University of Tsukuba, Ibaraki 305, Japan
(Received 10 April 1989)

Equilibrium charge distributions have been measured for 18 kinds of ions passing through a carbon foil in the energy region of 1–6 MeV/u for light ions and of 0.2–1 MeV/u for heavy ions. By combining the data obtained at present with those reported for other energies or ion species, an attempt is made to find the systematics for charge fraction $F(q)$, mean charge $\bar{q}$, and distribution width d over the wide range of ion species Z and energy E. Strong correlation has been found between the shell structure of ions and the variation of $\bar{q}$ or d with Z or E. The analysis for this correlation enables the evaluation of rather reliable values of $\bar{q}$, d, or $F(q)$ for ion species $4 \leq Z \leq 92$ in carbon foils from 0.02 to 6 MeV/u.

I. INTRODUCTION

The knowledge of the charge distribution of ions after the passage through matter is important not only for the study of atomic collision but also for its application to the design of nuclear instruments. Many authors have hitherto tried to find the systematic trend of charge fractions $F(q)$, mean charges $\bar{q}$, or charge distribution widths d, versus ion velocity v, ion species of atomic number Z, or target species.[1–14] Consequently, up to a few MeV/u and $Z \leq 36$, a rough estimation has become possible for $F(q)$, $\bar{q}$, or d values. Recently, in the ion energies of 0.02 to 2 MeV/u, we reported the presence of oscillation of $\bar{q}$ versus Z when equilibrium $\bar{q}$ values of various ions are compared at an equal velocity of ions in carbon foils.[15] This is a remarkable fact from the viewpoint of the scaling work of $F(q)$ that is characterized by two parameters of $\bar{q}$ and d. Because all the scaling works in the past have been done by assuming that the values $\bar{q}$ or d vary monotonically with the variation of Z or v, where the number of input data adopted for the scaling procedure was clearly insufficient. Necessarily, the $F(q)$ values evaluated by the use of $\bar{q}$ and d based on this assumption are accompanied by a significant deviation from observed values in some region of Z or v.

In this paper, an attempt is performed to find the systematics of $\bar{q}$ and d versus wide range of Z ($=4-92$) and of v or energy E ($=0.2-6$ MeV/u). Target material is limited to a carbon foil considering that the most abundant data are available for this target. Data sources in the present analysis are (a) data reported before 1985 compiled in two literatures,[16,17] (b) recent data[18–23] reported after 1985, and (c) new data obtained at present intending to complement the data of (a) and (b). New data include the equilibrium charge distributions of Be, B, C, O, Mg, Al, Si, Ca, Ti, Ga, Y, Rh, I, Nd, Ho, Ir, Au, and Bi ions around the 1-MeV/u energy region. Results show that the variation of $\bar{q}$ versus Z or v, as well as d versus Z or v is strongly correlated with the shell structure of ions. All data of d have proved to be scaled successfully with respect to mean number of electrons attached to ions, $Z-\bar{q}$. Present analysis for $\bar{q}$ and d enables one to evaluate rather reliable values of $F(q)$ over the wide range of Z and E.

II. EXPERIMENT AND RESULT

By using the 12 unit-double (UD) Pelletron tandem accelerator at the University of Tsukuba, equilibrium charge distributions were measured for ions ^{9}Be (1.2–5.3 MeV/u), ^{11}B (1.4–6.3), ^{12}C (2.0–6.3), ^{16}O (3.1–6.1), ^{24}Mg (0.8–3.8), ^{27}Al (0.5–3.6), ^{28}Si (4.1, 4.5), ^{40}Ca (0.4–3.1), ^{48}Ti (0.5–3.2), ^{69}Ga (0.5–1.9), ^{89}Y (0.6–1.7), ^{103}Rh (0.4–1.6), ^{127}I (0.4–1.1), ^{142}Nd (0.5–1.1), ^{165}Ho (0.3–1.0), ^{191}Ir (0.2–0.8), ^{197}Au (0.8), and ^{209}Bi (0.2–0.8) emerging from a carbon foil.

Experimental procedure for the measurement of $F(q)$ is described elsewhere.[24] A well-focused beam passed through a carbon foil (between 30 and 130 μg/cm^2) which is thick enough for the attainment of charge equilibration. The ions having charge state q behind the foil were charge analyzed by using a split-pole type magnetic spectrograph, and were collected with a Faraday cup connected to a current integrator. Elastically scattered ions or recoiled carbon ions were detected with a semiconductor detector whose counts during the run served to determine the charge fraction $F(q)$. Obtained data of $F(q)$ are to be analyzed with respect to the energies of ions at the emergence from foil.[17] Then, the energies were estimated from the knowledge of the incident energy and the projectile energy loss which is the product of stopping power and carbon foil thickness. This thickness was preliminarily measured using an ^{241}Am-α particle energy loss method. Judging from the statistics of the monitor detector counts and the reproducibility for the repeated measurements by using foils of different thickness, estimated maximum errors are less than 2.5% for $F(q)>0.08$, 8% for $F(q)>0.01$, and 18% for $F(q)<0.01$.

Obtained results of $F(q)$, mean charge $\bar{q}=\sum_q [qF(q)]$,

TABLE I. Equilibrium charge fraction $F(q)$, mean charge $\bar{q}$, and charge distribution width d for various ions passing through a carbon foil. $\bar{q}$ and d are in units of charge. The ion energy at the emergence from the foil is given in units of MeV/u.

Ion	Energy (MeV/u)	Mean Charge	Width	Charge fraction F(q) in %						
^{9}Be	E	$\bar{q}$	d	2+	3+	4+				
	1.285	3.78	0.44	0.97	20.0	79.0				
	1.623	3.87	0.35	0.30	12.7	87.0				
	2.181	3.93	0.25		6.63	93.4				
	2.745	3.967	0.18		3.27	96.7				
	3.303	3.978	0.15		2.24	97.8				
	3.860	3.987	0.11		1.29	98.7				
	4.412	3.992	0.091		0.83	99.17				
	5.306	3.995	0.066		0.46	99.54				
^{11}B	E	$\bar{q}$	d	3+	4+	5+				
	1.435	4.59	0.56	3.73	34.1	62.2				
	2.008	4.78	0.44	0.97	19.7	79.3				
	2.520	4.88	0.34	0.31	11.7	87.9				
	3.342	4.941	0.24		5.89	94.1				
	3.979	4.966	0.18		3.45	96.55				
	4.973	4.983	0.13		1.71	98.29				
	5.674	4.990	0.097		0.96	99.04				
^{10}B	6.249	4.992	0.091		0.83	99.17				
^{12}C	E	$\bar{q}$	d	4+	5+	6+				
	2.050	5.62	0.55	3.07	31.7	65.3				
	2.720	5.785	0.44	1.10	19.3	79.6				
	3.308	5.855	0.37	0.45	13.6	85.9				
	4.101	5.923	0.27	0.14	7.40	92.5				
	4.981	5.985	0.20	0.02	4.15	95.8				
	5.315	5.966	0.18		3.37	96.6				
	5.648	5.970	0.17		3.00	96.7				
	5.983	5.977	0.15		2.33	97.67				
	6.318	5.981	0.14		1.91	98.09				
^{16}O	E	$\bar{q}$	d	5+	6+	7+	8+			
	3.109	7.59	0.58	0.09	4.35	32.6	63.0			
	3.610	7.70	0.51		2.35	25.8	71.8			
	4.112	7.78	0.45		1.25	19.7	79.0			
	4.613	7.83	0.39		0.66	15.6	83.7			
	5.103	7.87	0.35		0.40	12.0	87.6			
	5.591	7.902	0.30		0.19	9.38	90.43			
	6.093	7.925	0.27		0.09	7.27	92.64			
^{24}Mg	E	$\bar{q}$	d	6+	7+	8+	9+	10+	11+	12+
	0.842	8.61	1.03	2.08	11.9	30.5	35.3	18.9	1.32	
	0.994	9.00	0.96		6.44	23.5	37.3	29.3	3.40	
	1.415	9.56	0.94		1.65	11.0	31.2	42.7	12.4	0.99
	2.034	10.20	0.88			2.88	16.1	45.0	30.2	5.80
	2.457	10.54	0.86			1.09	9.01	37.1	40.6	12.3
	2.877	10.80	0.82			0.38	4.72	29.1	45.8	20.0
	3.061	10.90	0.82			0.27	3.87	25.9	45.4	24.5
	3.271	11.01	0.80			0.16	2.82	21.8	46.3	28.9
	3.479	11.13	0.74				0.91	19.0	46.6	33.5
	3.692	11.19	0.74				1.43	15.8	45.6	37.2
	3.818	11.23	0.73				1.19	14.5	44.6	39.6
^{27}Al	E	$\bar{q}$	d	5+	6+	7+	8+	9+	10+	11+	12+	13+
	0.537	8.07	1.00		5.73	22.4	37.9	26.9	7.06			
	0.708	8.61	1.08	0.21	2.12	12.1	31.0	34.7	16.4	3.46		
	1.081	9.59	1.06		0.23	2.40	12.0	30.5	34.9	18.3	1.57	
	1.361	10.08	1.02			0.75	5.84	20.7	35.8	31.5	5.14	0.26
	2.043	10.86	0.93				0.79	6.36	24.5	45.6	20.1	2.69
	2.551	11.38	0.89				0.16	1.91	12.4	40.6	35.7	9.25
	3.110	11.72	0.85					0.67	6.30	31.6	43.4	18.0
	3.594	11.97	0.79						3.36	22.6	47.5	26.5
^{28}Si	E	$\bar{q}$	d	10+	11+	12+	13+	14+		
	4.048	12.98	0.81	0.08	3.33	23.2	45.6	27.8		
	4.432	13.08	0.79		2.82	19.0	45.5	32.7		
	4.552	13.22	0.72		0.57	16.0	44.9	38.6		
^{32}S	E	$\bar{q}$	d	7+	8+	9+	10+	11+	12+	13+	14+
	0.998	10.67	1.14	0.29	2.36	11.7	29.1	33.9	17.8	4.34	0.51

TABLE I. (*Continued.*)

Ion	Energy (MeV/u)	Mean Charge	Width	Charge fraction F(q) in %															
	E	$\bar{q}$	d	8+	9+	10+	11+	12+	13+	14+	15+	16+	17+	18+	19+				
^{40}Ca	0.450	10.87	1.20	2.49	9.33	26.2	32.7	21.0	6.95	1.33									
	0.549	11.43	1.20	0.59	3.36	18.1	31.0	29.3	13.7	3.53	0.53								
	0.716	12.06	1.24		1.44	8.62	22.7	31.7	23.4	9.55	2.50								
	1.015	12.90	1.24		0.23	2.36	10.1	23.9	31.9	22.2	8.08	1.23	0.07						
	1.438	13.93	1.22			0.24	2.15	9.34	23.4	32.7	23.3	7.71	1.21	0.06					
	1.992	14.99	1.20				0.19	1.79	8.32	22.6	33.1	24.5	8.26	1.18	0.02				
	2.445	15.70	1.17					0.35	2.68	11.4	27.7	33.4	19.1	5.14	0.28				
	2.888	16.22	1.13						0.79	4.98	20.4	33.0	28.3	11.4	1.16				
	3.140	16.53	1.08							3.15	13.7	31.1	33.7	16.2	2.13				
	E	$\bar{q}$	d	8+	9+	10+	11+	12+	13+	14+	15+	16+	17+	18+	19+	20+	21+		
^{48}Ti	0.539	12.50	1.25	0.20	1.13	4.29	13.1	31.0	30.1	15.5	4.12	0.58	0.04						
	0.695	13.20	1.23		0.25	1.40	5.89	20.4	31.0	28.0	10.5	2.34	0.25						
	1.009	14.15	1.27			0.19	1.33	7.92	20.5	30.9	25.1	11.3	2.59	0.24					
	1.324	14.92	1.27				0.26	2.43	10.3	23.7	30.6	22.5	8.60	1.46	0.09				
	1.616	15.56	1.27					0.73	4.38	14.9	27.8	28.8	18.0	4.89	0.49				
	2.030	16.35	1.22					0.08	1.01	5.50	16.6	30.3	29.7	13.9	2.67	0.19			
	2.450	17.00	1.19						0.19	1.74	8.21	22.3	33.6	24.6	8.21	1.10	0.03		
	2.870	17.58	1.16							0.49	3.21	13.1	29.1	33.0	17.3	3.57	0.17		
	3.184	17.95	1.12								1.49	8.39	23.0	35.7	23.9	7.00	0.45		
	E	$\bar{q}$	d	10+	11+	12+	13+	14+	15+	16+	17+	18+							
^{52}Cr	0.551	13.69	1.28	1.12	4.26	11.6	22.7	35.2	18.8	5.49	0.78	0.06							
	E	$\bar{q}$	d	11+	12+	13+	14+	15+	16+	17+									
^{55}Mn	0.524	13.99	1.33	4.23	9.78	20.1	26.8	28.2	8.99	1.83									
	E	$\bar{q}$	d	10+	11+	12+	13+	14+	15+	16+	17+	18+	19+						
^{59}Co	0.581	14.95	1.54	0.17	1.26	4.46	11.6	20.1	24.8	20.3	14.4	2.49	0.28						
	E	$\bar{q}$	d	11+	12+	13+	14+	15+	16+	17+	18+	19+	20+	21+	22+	23+	24+	25+	26+
^{69}Ga	0.552	15.23	1.66	0.80	3.33	10.5	19.2	24.4	20.3	12.6	6.16	2.25	0.72						
	1.000	18.48	1.75				0.24	1.10	3.77	8.50	14.8	20.3	21.2	17.3	10.6	1.91	0.28	0.03	
	1.945	22.01	1.37							0.14	0.66	2.61	7.91	23.9	30.0	21.3	10.2	2.75	0.38
	E	$\bar{q}$	d	12+	13+	14+	15+	16+	17+	18+	19+	20+	21+	22+	23+	24+	25+	26+	27+	28+
^{75}As	0.560	15.62	1.56	1.81	6.82	15.6	23.5	23.4	16.6	8.78	3.46									
	1.944	23.04	1.47							0.32	1.15	3.52	8.98	17.5	31.5	22.6	10.7	3.13	0.55	0.06

TABLE I. (*Continued.*)

Ion	Energy (MeV/u)	Mean Charge	Width	Charge fraction F(q) in %																		
	E	$\bar{q}$	d	13+	14+	15+	16+	17+	18+	19+	20+	21+	22+	23+	24+	25+	26+	27+	28+	29+	30+	
^{89}Y	0.581	18.09	1.71	0.27	1.41	4.61	11.2	18.6	22.8	20.9	12.7	5.42	1.62	0.35	0.06							
	0.692	18.79	1.73	0.07	0.48	2.11	6.51	13.7	20.1	23.5	17.8	10.2	4.06	1.19	0.26	0.05						
	0.837	19.70	1.77		0.11	0.60	2.66	7.03	13.7	22.0	21.8	17.1	9.51	3.88	1.26	0.30	0.07					
	0.994	20.62	1.80				0.91	2.78	7.64	15.3	21.6	21.5	15.7	8.90	4.04	1.24	0.26					
	1.137	21.32	1.87				0.29	1.27	4.18	10.2	18.3	21.6	18.1	13.6	7.68	3.32	1.19	0.28	0.05			
	1.329	22.41	1.98					0.32	1.48	4.90	10.0	16.7	18.7	19.1	14.0	8.61	4.22	1.47	0.44	0.08		
	1.565	23.73	2.00						0.28	1.18	3.65	8.21	14.1	18.1	19.3	16.1	10.8	5.62	2.07	0.61	0.04	
	1.701	24.40	1.98							0.49	1.83	4.93	10.1	15.4	18.8	18.8	14.9	9.15	4.09	1.38	0.15	
	E	$\bar{q}$	d	16+	17+	18+	19+	20+	21+	22+	23+	24+	25+	26+	27+	28+	29+	30+	31+	32+		
^{103}Rh	0.412	19.42	1.46	1.72	7.76	17.1	25.9	24.9	14.8	6.08	1.70											
	0.605	21.21	1.61	0.11	0.74	3.37	9.74	19.3	24.4	21.5	13.4	5.47	1.57	0.31	0.05							
	0.795	22.30	1.69		0.06	0.80	3.56	10.0	18.2	21.8	21.6	14.6	6.50	2.28	0.52							
	0.989	23.37	1.71				0.90	3.50	9.30	17.2	22.1	21.4	15.0	7.23	2.61	0.68						
	0.992	23.50	1.72				0.76	3.11	8.44	15.8	22.1	22.2	15.8	7.87	3.05	0.81	0.18					
	1.213	24.45	1.79				0.12	0.94	3.46	9.00	16.9	20.9	20.7	15.3	8.23	3.17	0.96	0.22				
	1.459	25.62	1.83					0.19	0.88	3.06	8.03	14.9	20.9	21.1	16.1	9.13	3.99	1.36	0.35	0.07		
	1.561	26.01	1.86					0.10	0.51	2.08	5.74	12.1	19.1	21.4	18.4	11.9	5.81	2.31	0.69	0.16		
	1.583	26.13	1.86						0.37	1.78	5.38	11.2	18.3	21.5	18.7	12.6	6.55	2.59	0.79	0.20		
	E	$\bar{q}$	d	17+	18+	19+	20+	21+	22+	23+	24+	25+	26+	27+	28+	29+	30+	31+				
^{115}In	0.609	22.32	1.54	0.14	0.65	2.59	6.89	18.9	26.4	23.3	13.7	5.59	1.55	0.35								
	0.999	25.32	1.70				0.13	0.81	3.38	9.35	18.0	23.3	21.3	13.4	6.99	2.51	0.59	0.14				
	E	$\bar{q}$	d	14+	15+	16+	17+	18+	19+	20+	21+	22+	23+	24+	25+	26+	27+	28+	29+	30+	31+	32+	33+
^{127}I	0.356	20.18	2.09	0.28	1.05	2.75	5.82	11.0	16.3	18.3	17.4	13.6	8.25	3.63	1.29	0.28						
	0.423	21.45	2.10		0.27	0.93	2.35	4.91	8.99	14.2	17.9	18.4	15.5	9.79	5.01	1.47	0.27					
	0.499	22.72	1.98			0.21	0.65	1.67	3.74	7.12	12.0	17.3	21.0	17.6	12.6	4.84	1.21	0.23				
	0.551	23.42	1.84				0.18	0.59	1.72	4.00	8.05	14.3	20.9	21.4	17.5	8.14	2.69	0.61	0.12			
	0.630	24.12	1.76					0.17	0.58	1.78	4.57	10.4	16.8	21.5	23.5	13.1	5.38	1.77	0.38			
	0.708	24.75	1.74						0.21	0.84	2.60	6.58	12.3	18.6	25.3	19.2	9.54	3.64	0.98	0.20		
	0.823	25.72	1.65							0.16	0.62	1.95	5.63	12.6	23.7	24.5	17.6	8.79	3.26	0.96	0.21	
	0.982	26.75	1.70								0.13	0.54	1.99	5.71	14.1	22.0	23.2	17.6	9.49	3.74	1.20	0.27
	1.123	27.92	1.76										0.55	1.92	5.93	12.4	19.4	23.5	18.0	11.2	4.98	1.64	0.44
	E	$\bar{q}$	d	18+	19+	20+	21+	22+	23+	24+	25+	26+	27+	28+	29+	30+	31+	32+	33+			
^{139}La	0.553	23.77	2.27	0.65	2.11	4.80	9.03	13.4	15.4	16.4	14.5	11.5	7.56	3.22	1.11							
	0.871	27.18	2.02				0.49	1.28	2.86	5.60	9.49	14.3	19.8	19.1	15.9	7.91	2.45	0.67	0.12			
	E	$\bar{q}$	d	18+	19+	20+	21+	22+	23+	24+	25+	26+	27+	28+	29+	30+	31+	32+	33+	34+		
^{142}Nd	0.541	23.70	2.36	0.78	2.26	5.28	9.66	13.5	16.6	16.1	13.6	9.66	6.37	3.67	1.80	0.71						
	0.645	25.07	2.35			2.00	4.28	7.67	12.0	15.7	16.9	14.4	11.0	7.77	4.94	2.43	0.94					
	0.749	26.29	2.37				1.71	4.06	6.89	11.1	14.4	15.2	14.8	13.1	9.44	5.95	2.65	0.96				
	0.886	27.75	2.36					1.23	3.05	5.38	8.54	11.7	14.9	15.6	15.1	12.5	7.51	3.61	1.12			
	0.970	28.52	2.31					0.50	1.53	3.23	5.74	8.44	12.3	15.0	16.9	16.1	11.2	6.35	2.13	0.51		
	1.050	29.27	2.13							1.64	3.42	6.28	9.47	13.5	16.9	18.9	14.9	9.93	3.99	1.07		

TABLE I. (*Continued.*)

Ion	Energy (MeV/u)	Mean Charge	Width	Charge fraction F(q) in %																								
^{165}Ho	E	$\bar{q}$	d	16+	17+	18+	19+	20+	21+	22+	23+	24+	25+	26+	27+	28+	29+	30+	31+	32+	33+	34+	35+	36+				
	0.309	21.18	2.03	0.90	2.45	5.86	10.9	16.9	19.6	17.8	13.2	7.22	3.42	1.33	0.45													
	0.435	23.49	2.13			0.67	2.01	5.04	9.74	14.9	18.9	17.7	13.6	9.49	4.80	2.12	0.84	0.29										
	0.549	25.03	2.21				0.40	1.24	3.49	7.25	12.6	16.4	17.5	15.8	11.8	7.16	3.87	1.70	0.66										
	0.824	27.92	2.42							0.69	2.01	4.58	8.40	13.2	15.7	15.9	14.4	10.8	6.87	3.97	2.22	0.95	0.38					
	0.896	28.62	2.51							0.44	1.18	2.88	5.73	9.97	13.5	15.4	15.5	13.2	9.51	5.97	3.60	1.84	0.87	0.35				
	0.962	29.29	2.49									1.81	3.98	7.15	11.2	13.8	15.4	15.4	11.7	8.64	5.47	2.94	1.41	0.60				
^{175}Lu	E	$\bar{q}$	d	20+	21+	22+	23+	24+	25+	26+	27+	28+	29+	30+	31+	32+	33+	34+	35+	36+								
	0.551	26.32	2.10	0.22	0.74	2.28	5.46	10.4	16.1	18.9	17.7	13.7	8.00	4.04	1.74	0.59	0.19											
	0.876	29.46	2.27					0.92	2.52	5.80	10.4	15.1	17.0	16.6	13.3	8.96	5.06	2.65	1.18	0.46								
^{191}Ir	E	$\bar{q}$	d	15+	16+	17+	18+	19+	20+	21+	22+	23+	24+	25+	26+	27+	28+	29+	30+	31+	32+	33+	34+	35+	36+	37+		
	0.226	20.78	2.28	0.74	2.20	4.69	8.51	13.0	15.8	17.5	14.8	11.0	6.82	3.24	1.37	0.42												
	0.349	24.70	2.19				0.23	0.75	1.95	4.48	8.45	12.7	17.4	17.7	15.6	10.9	5.99	2.74	0.86	0.23								
	0.451	26.77	1.99								1.33	3.51	7.74	14.1	18.5	19.5	15.5	11.0	5.71	2.37	0.68							
	0.560	28.28	2.06								0.21	0.73	2.20	5.42	10.6	16.1	19.3	18.1	13.7	7.79	3.89	1.59	0.47					
	0.656	29.30	2.03										0.71	2.15	5.43	10.6	15.8	20.0	18.0	13.4	7.96	3.92	1.52	0.51				
	0.779	30.59	2.07											0.50	1.69	4.43	8.86	14.7	18.6	18.6	15.1	9.65	4.80	2.07	0.80	0.25		
^{197}Au	E	$\bar{q}$	d	26+	27+	28+	29+	30+	31+	32+	33+	34+	35+	36+	37+													
	0.822	31.58	2.04	0.52	1.63	4.40	8.80	14.6	18.7	18.3	15.5	9.88	4.78	2.05	0.70													
^{209}Bi	E	$\bar{q}$	d	15+	16+	17+	18+	19+	20+	21+	22+	23+	24+	25+	26+	27+	28+	29+	30+	31+	32+	33+	34+	35+	36+	37+		
	0.191	20.22	2.17	1.01	2.97	6.61	11.0	15.6	18.6	17.4	12.4	7.60	4.20	1.92	0.76													
	0.277	23.78	2.25				0.54	1.64	4.27	9.04	14.3	17.0	16.6	14.6	10.1	6.43	3.33	1.43	0.52	0.16								
	0.367	26.59	2.23							0.82	2.30	5.23	9.57	13.5	16.8	17.5	14.3	9.99	6.07	2.57	0.97	0.26						
	0.460	28.51	2.19								0.25	0.81	2.49	5.05	9.34	14.3	17.6	17.3	14.6	9.68	5.53	2.20	0.73	0.18				
	0.554	29.92	2.10										0.44	1.35	3.51	7.69	12.2	16.1	19.0	16.9	12.3	6.65	2.66	0.99	0.29			
	0.648	31.05	2.04												1.17	3.14	6.27	11.6	17.0	19.6	17.9	12.1	6.67	3.07	1.17	0.35		
				27+	28+	29+	30+	31+	32+	33+	34+	35+	36+	37+	38+													
	0.767	32.27	2.07	0.87	2.48	5.51	10.6	15.8	19.7	18.0	12.8	8.11	4.08	1.52	0.56													
	0.827	32.82	2.01		1.29	3.61	7.70	13.1	18.5	19.6	15.9	10.6	6.02	2.73	0.88													

and charge distribution width $d=[\sum_q (q-\bar{q})^2 F(q)]^{1/2}$ are listed in Table I for each emergent energy E in units of MeV/u. Table I includes the data of S, Cr, Mn, Co, As, In, La, or Lu ions other than those mentioned above. For these ions, only $\bar{q}$ values were graphically displayed in our previous paper[15] reporting the Z oscillation of $\bar{q}$.

III. MEAN CHARGE $\bar{q}$

As early as 1948, by applying the Thomas-Fermi atomic model to the projectile's electrons, Bohr[25] presented an expression for mean charges of ions produced by a single collision with an atom as

$$\bar{q}/Z = v/(v_0 Z^{2/3}) , \quad (1)$$

where v_0 represents the Bohr velocity. Its derivation is based on the criterion that the ionic bound electrons are lost in a collision when their velocity is below v. Although Eq. (1) is not adequate to apply to the equilibrium $\bar{q}$ of ions in solid target, Bohr's criterion has become a fundamental concept in considering the $\bar{q}$ values of ions in matter. In fact, in the scaling work of $\bar{q}$ versus Z and v, many authors have adopted more or less the modified function of Eq. (1) as the scaling variable. For instance, semiempirical or empirical formulas for $\bar{q}$ of ions in carbon foils by Nikolaev and Dmitriev[3] (ND), To and Drouin[4] (TD), and Shima *et al.*[8] (SIM) were obtained by taking the scaling variable X as

$$X = v/(v' Z^{0.45}), \quad v' = 3.6\times 10^8 \text{ cm/sec} , \quad (2)$$

and their formulas are given by

$$\text{ND: } \bar{q}/Z = (1+X^{-5/3})^{-3/5} \text{ for } 0.3 < q/Z < 0.7 , \quad (3)$$

$$\text{TD: } \bar{q}/Z = 1-\exp(-X) , \quad (4)$$

$$\text{SIM: } \bar{q}/Z = 1-\exp(-1.25+0.32X-0.11X^2) \text{ for } X < 2.4 . \quad (5)$$

Similar expressions of $\bar{q}$ of ions in carbon foils are presented by Betz,[2] Baron,[6] and Sayer.[7] Each formula is valid within the framework of limited data sources adopted in its derivation. These formulas in common suggest the trend of the monotonic increase of $\bar{q}$ with increasing Z for given value of v, or with increasing v for given value of Z. This situation, however, has changed dramatically through the recent data accumulation including the data of Table I—the appearance of the oscillation of $\bar{q}$ versus Z or v.

A. Oscillation of $\bar{q}$ versus Z and v

An oscillatory behavior of $\bar{q}$ with Z is shown in Fig. 1 where $\bar{q}/Z$ values are compared at an equal velocity of ions. Original data were taken in the vicinity (within 22%) of 0.02 (Refs. 26 and 27), 0.1, 0.55, 1, 2, 4, and 6 MeV/u. Meanwhile, plotted data points are those after correction. Namely, because of the necessity that the $\bar{q}$ values are to be compared at a common exit velocity of ions from the foil, each original $\bar{q}$ value was extrapolated to that of the common velocity by employing an empirical relation of $\bar{q}$ versus v given by Eq. (4). Dotted curves

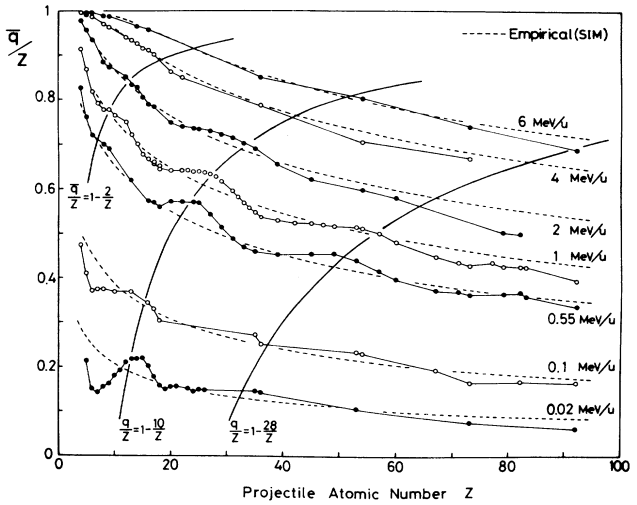

FIG. 1. Equilibrium mean charges $\bar{q}$ divided by atomic number of ions Z plotted against Z for ions after passage through a carbon foil. Plotted data points are the values after correction from the original $\bar{q}$ values so that the $\bar{q}$ values of various ion species may be compared at an equal velocity of ions, because original data are not always taken at an exact value of ion energies quoted in the figure (see text). Thin solid lines connecting the data points are drawn to guide the eye. Dashed lines indicate the values from an empirical formula by Shima *et al.* given by Eq. (5). Explanation for thick solid curves denoted with $\bar{q}/Z = 1-2/Z$, $1-10/Z$, and $1-28/Z$ is given in the text.

show the empirical relation of $\bar{q}$ versus Z by SIM [Eq. (5)], showing general agreement with observed values apart from the oscillation of $\bar{q}$.

The origin of the Z oscillation of $\bar{q}$ was already discussed in our previous paper,[15] and hence, only an essential point is described here. An important fact is that the mean ionization potential potential of ions having mean charge state $\bar{q}$ was found to oscillate as a function of Z. Based on this data, one of the origins of the Z oscillation of $\bar{q}$ is attributed to the Z oscillation of electron loss as well as electron capture cross section of ions. Another possibility is in the Z oscillation of the post-foil Auger-electron emission yield.

Figure 1 indicates that the Z oscillatory phase varies according to the variation of v, and its amplitude gradually diminishes with increasing v. It was pointed out in our previous paper[15] that the enhancement of $\bar{q}$ takes place for ions having the closed-shell structure on an average. In other words, the maxima of the Z oscillation of $\bar{q}$ take place for ions whose mean number of electrons $\bar{n_e} = Z-\bar{q}$ corresponds to 2 (He-like ions with full K-shell electrons), 10 (Ne-like ions with full L-shell electrons), and 28 (Ni-like ions with full M-shell electrons). In fact, if we draw the relation $\bar{q}/Z = 1-2/Z$, $1-10/Z$, and $1-28/Z$ in Fig. 1 (solid curves), the contour map of $\bar{q}/Z$ versus Z is seen to be characterized by these three curves from low-velocity ions of 0.02 MeV/u up to at least several MeV/u. Although another enhancement of $\bar{q}$ is expected to occur along the curve $\bar{q}/Z = 1-46/Z$ for $4d$ core ions having 46 electrons, we can afford no definite

conclusion on this point within the framework of the data in Fig. 1.

It naturally follows from the oscillation of $\bar{q}$ versus Z for each given v in Fig. 1 that the similar oscillation is present for $\bar{q}$ versus v when Z is given. Figure 2 displays the experimental $\bar{q}$ values of Br ions plotted against v together with an empirical relation by TD [Eq. (4)]. The empirical $\bar{q}$ values increase monotonically with increasing v, meanwhile observed $\bar{q}$ values exhibit some structure which turns out to be a part of oscillation. This is because the $\bar{q}$ values enhance at the ion velocities corresponding to the Ne-like ions ($\bar{q}=Z-10$) and Ni-like ions ($\bar{q}=Z-28$). The argument mentioned above is not specific to Br ions but is general for other ions.

Under the choice of a scaling variable like Eq. (2) that is a monotonic function of Z or v, Figs. 1 and 2 suggest that the scaling of $\bar{q}$ is inherently accompanied by the scattering of data around the scaled curve.

B. Mean charges of highly charged ions

Apart from the deviation accompanied by the oscillation of $\bar{q}$ versus Z or v, an empirical formula by SIM is known to be applicable to ions of relatively high-velocity region[8] since it was derived from the data of $Z \geq 14$ and $X < 2.4$. Above $X \cong 2.4$ or $\bar{q}/Z > 0.93$ [see Eq. (5)], there is no empirical relation and the data are scarce. Then, within the framework of existing data, the systematics of $\bar{q}$ for such highly charged ions is considered in the following.

Using the scaling variable X given by Eq. (2), all existing data for $Z \geq 4$ and $X > 1.8$ are shown in Fig. 3. In addition to the data of light ions mostly taken from Table I, the data of 11.5 MeV/u Ar ions[28] and 15.6 MeV/u Ni ions[18] are included. Empirical relations by SIM at $X < 2.4$ and ND and TD at $X < 2$ are also drawn. The ordinate $\ln(1-\bar{q}/Z)$ is taken to emphasize the variation of $\bar{q}/Z$ values approaching the unit value. At $X > 3$, the values $(1-\bar{q}/Z)$ are seen to be proportional approximately to $\exp(-X)$. In this region, the consideration on the oscillation of $\bar{q}$ versus Z or v is no longer necessary, because observed charge fractions are dominated by fully stripped ions of $q=Z$ and H-like ions of $q=Z-1$.

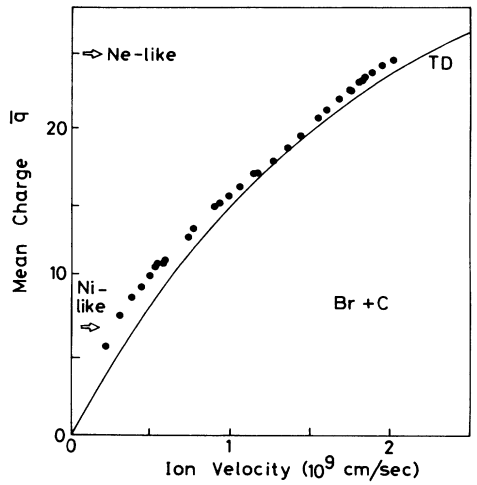

FIG. 2. Equilibrium mean charges of Br ions after passage through a carbon foil. Solid curve indicates an empirical relation given by To and Drouin (TD) in Eq. (4).

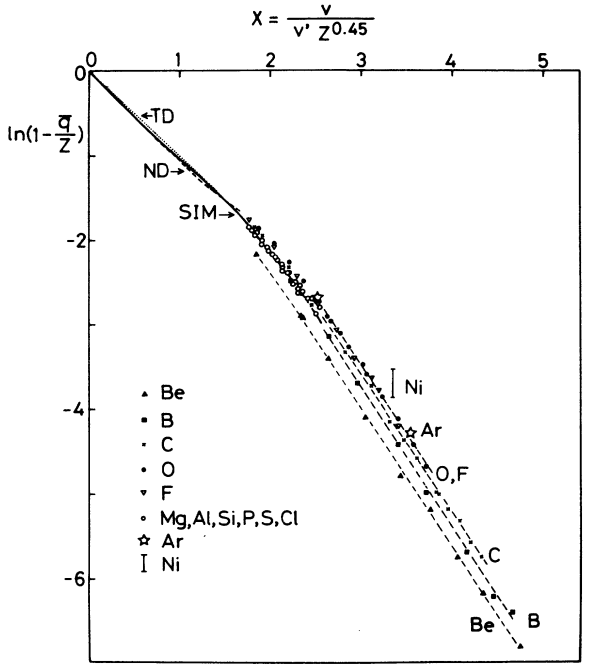

FIG. 3. Velocity dependence of equilibrium mean charges of highly charged ions. The velocity parameter X is given by Eq. (2).

For charge equilibrium ions having only two components of $q=Z$ and $q=Z-1$, we obtain

$$\bar{q}=ZF(Z)+(Z-1)F(Z-1)\ , \tag{6}$$

$$\sigma_1 F(Z-1)=\sigma_c F(Z)\ , \tag{7}$$

where σ_1 and σ_c, respectively, denote the electron-loss cross sections for H-like ions and electron-capture cross sections for fully stripped ions. In this case, the ordinate of Fig. 3 reduces to $\ln(1-\bar{q}/Z)=\ln[F(Z-1)/Z]$. Regarding the data of $F(Z)+F(Z+1)>0.97$ being in conformity with the two-component condition, all those data are plotted in Fig. 4 by adopting new coordinates of $\ln[F(Z-1)/Z]-A$ and

$$X'=143Z^{-0.48}\beta/(1-\beta^2)^{1/2}\ ,$$

where $\beta=v/c$. The data points are seen to be approximated by a straight line given by

$$\ln[F(Z-1)/Z]=A-X'\ , \tag{8}$$

where

$$A=0.67(Z-3)^{0.183}+0.3\ . \tag{9}$$

From Eqs. (6) to (8) we obtain

$$F(Z)/F(Z-1)=\sigma_1/\sigma_c=\exp(-A+X')/Z-1\ , \tag{10}$$

$$F(Z-1)=1-F(Z)=Z\exp(A-X')\ . \tag{11}$$

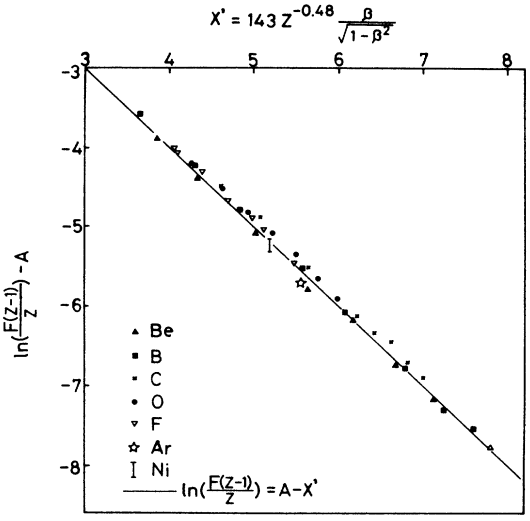

FIG. 4. Velocity dependence of equilibrium mean charges of highly charged ions where the value $F(Z)+F(Z-1)$ exceeds 97%. Abscissa indicates the velocity parameter $X'=143Z^{-0.48}\beta/(1-\beta^2)^{1/2}$, where $\beta=v/c$, and the ordinate is $\ln[F(Z-1)/Z]-A$, where $A=0.67(Z-3)^{0.18}+0.3$. Solid straight line is an empirical relation expressed by $F(Z-1)/Z=\exp(A-X')$.

Equation (11) is an asymptotic function of $F(Z)$ or $F(Z-1)$ for highly charged ions of $4\leq Z\leq 18$ and $X>3$. There are many theoretical investigations on charge exchange cross sections of H-like ions and fully stripped ions. An experimental cross-section ratio given by Eq. (10) would be useful to test the validity of those theoretical works.

IV. CHARGE DISTRIBUTION WIDTH

Charge distribution width d corresponds to the standard deviation when the distribution function is Gaussian. Physically, as was described by Betz,[1,2] it is understood that the d values are related to the magnitudes of n and n' if we accept the condition that (a) $F(q)$ is Gaussian, (b) single-electron transfer is dominant, and (c) electron-loss and -capture cross sections are, respectively, given by $\sigma_{q,q+1}\propto q^{-n}$ and $\sigma_{q+1,q}\propto q^{n'}$, where the notation (q,q') denotes the charge exchange from charge state q to q'. Under the above conditions, Betz[2] mentioned that the d value is approximated by $[\bar{q}/(n+n')]^{1/2}$.

For equilibrium charge ions passing through a carbon foil, there exist several semiempirical or empirical formulas of d. Representative ones are

$$d=0.5\,\bar{q}^{1/2}(1-\bar{q}/Z)^{5/6} \tag{12}$$

by Nikolaev and Dmitriev[3] (ND) and

$$d=1.41Z^{0.11}\bar{q}^{0.3}(1-\bar{q}/Z)^{0.37} \tag{13}$$

by Betz.[2] Other expressions are given by Sayer[7] and Baudinet-Robinet.[13] These formulas suggest that the d values are a monotonically varying function of Z or v if $\bar{q}$ does not oscillate versus Z or v.

A. Z and v dependence of d

Z dependence of d is shown in Fig. 5 for low-velocity ions (0.02 MeV/u) and high-velocity ions (1 MeV/u). For comparison, the semiempirical relation[3] of ND [Eq. (12) or (14)] is drawn with solid curves. Experimental d values exhibit an oscillatory behavior with Z where the oscillation of d for 0.02 MeV/u ions was already reported by Lennard *et al.*[27] leaving its explanation unclarified. Indicated in the figure is the ionic shell which retains an outermost electron of ions having mean charge $\bar{q}$ at the moment when each d value is observed. It is clear that there exists some correlation between the shell structure of ions and the Z oscillation of d. Because each cycle of oscillation is followed in common by the appearance of different shell or subshell regardless of the ion velocity.

Figure 6 shows the v dependence of d for several ion species ranging from $Z=17$ to 83. Data are plotted by adopting the coordinates $d/Z^{1/2}$ and $X=v/(v'Z^{0.45})$ [Eq. (2)] so that they may focus along the semiempirical relation by ND (drawn with a solid curve) obtained from Eqs. (3) and (12) as

$$d/Z^{1/2}=0.5X^{-5/6}(1+X^{-5/3})^{-0.8}\,. \tag{14}$$

Figure 6 suggests that X is a poor variable for the scaling of d. The variation of experimental d versus v is not a monotonic function of X or v, and each complicated curve of d versus v appears to have no regularity when compared among different ion species. As a matter of fact, all these curves can be scaled (see Sec. IV B), and turn out to be a part of the oscillation of d versus v. Prior to describing this, we will first consider the meaning of

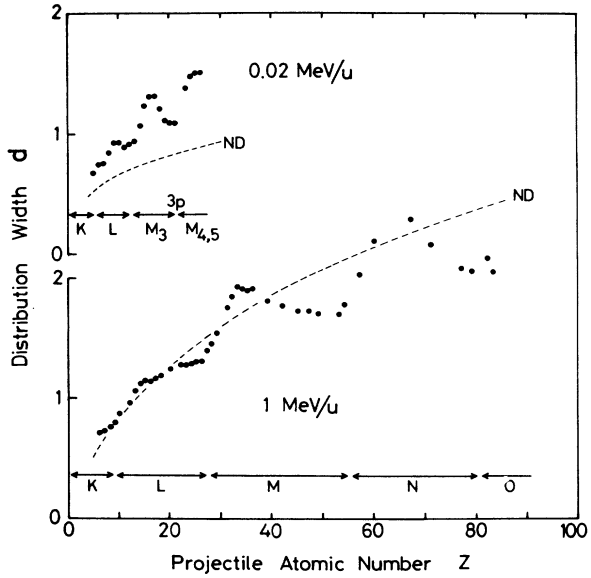

FIG. 5. Charge distribution width d of ions observed at 0.02 and 1 MeV/u vs atomic number of ions Z. ND stands for the empirical d values by Nikolaev and Dmitriev given by Eq. (14). K, L, M, N, or O indicates the ionic shell which retains the outermost electrons of ions having mean charge $\bar{q}$ when each d value is observed in the charge distribution.

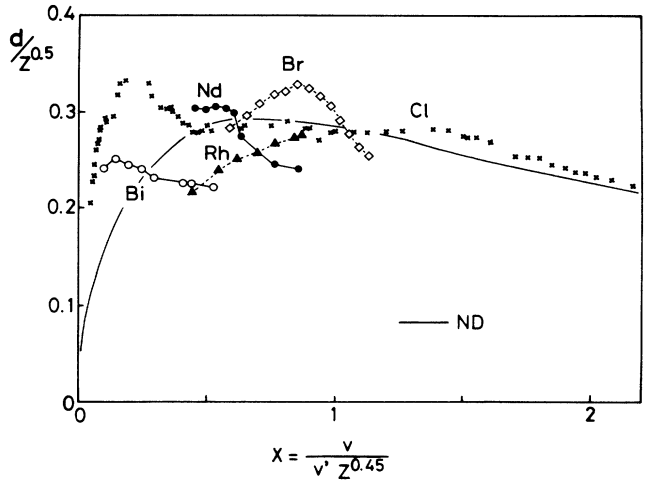

FIG. 6. Velocity dependence of charge distribution width d of several ions after the passage through a carbon foil. The velocity parameter X is given by Eq. (2). ND stands for the empirical d values given by Eq. (14).

the variation of d versus v in connection with the variation of $F(q)$.

When the charge distribution is Gaussian, the ratio of $F(q)$ between adjacent charge states $q+1$ and q is given by

$$\ln[F(q+1)/F(q)] = -q/d^2 + (\bar{q} - 0.5)/d^2 , \quad (15)$$

which means that, in the plot of $\ln[F(q+1)/F(q)]$ as a function of q, the slope $-1/d^2$ indicates a measure for the magnitude of d. In Figs. 7(a), 7(b), and 7(c), d versus ion energy, $F(q)$ values versus ion energy, and charge fraction ratios are, respectively, plotted for Cu ions observed after passage through a carbon foil. The difference of the slope occurred at the boundary of Ne-like ions ($q=19$) seen in Fig. 7(c) is the phenomenon known as the shell effect of $F(q)$ first reported by Moak *et al.*[29] From the magnitudes of the slope in Fig. 7(c) and Eq. (15), it is understood that the d values of the group $q \geq 19$ are lower than those $q \leq 18$. Namely, the d values of charge distribution in which outermost electrons are distributed mainly in the L shell are lower than those mainly in the M shell; meanwhile the d values take the intermediate values for $F(q)$ which is composed of outermost electrons distributed both in L and M shells. This behavior is displayed in Fig. 7(a). For the relation of

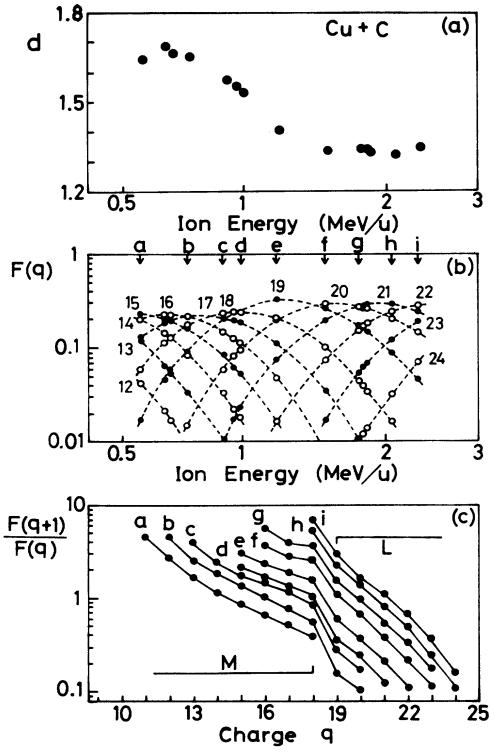

FIG. 7. Relationship between the charge distribution width vs ion energy and the charge fraction versus ion energy for Cu ions. (a) Charge distribution width d. (b) Charge fraction $F(q)$ for charge states $q=12$ to 24. (c) Charge fraction ratio between adjacent charge states $F(q+1)/F(q)$ vs charge state q at several ion energies of a to i as indicated in (b). L and M indicate the ionic shells which retain the outermost electron of ions with charge state q.

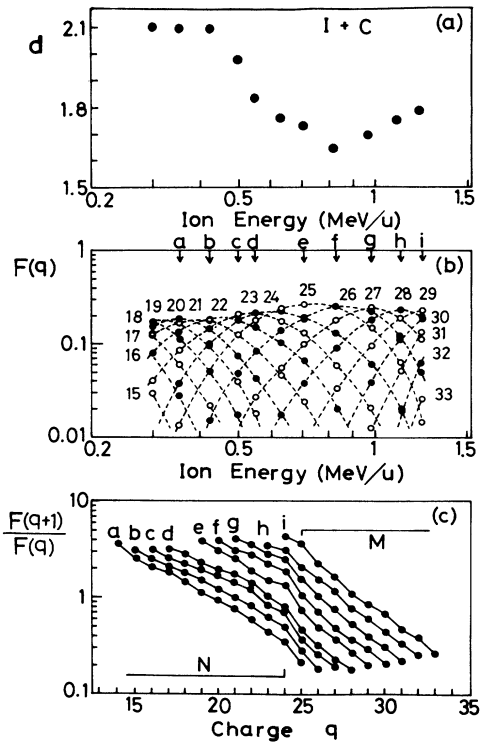

FIG. 8. Relationship between the charge distribution width vs ion energy and the charge fraction versus ion energy for I ions. (a) Charge distribution width d. (b) Charge fraction $F(q)$ for charge states $q=15$ to 33. (c) Charge fraction ratio between adjacent charge states $F(q+1)/F(q)$ vs charge state q at several ion energies of a to i as indicated in (b). M and N indicate the ionic shells which retain the outermost electron of ions with charge state q.

$F(q)$ versus ion energy in Fig. 7(b), it should be noted that the envelope connecting the maxima of each $F(q)$ curves jumps at the boundary charge state of Ne-like ions ($q=19$). This corresponds to the fact that the d value of $F(q)$ composed of L electrons are lower than that composed of M electrons. Thus, the variation of d versus v or ion energy is understood to be correlated with the variation of the projectile shell which retains the outermost electron of ions with $q \cong \bar{q}$.

Figure 8 shows the data of I ions where the presence of the similar trend is recognized even at the boundary charge state of Ni-like ions (data are taken from Table I and Ref. 30). In this case, the shell effect of $F(q)$ takes place between the group of ions $q \geq 25$ and $q \leq 24$ [see Fig. 8(c)], and the envelope connecting the maxima of $F(q)$ curves in Fig. 8(b) is seen to enhance at $q=25$ which corresponds to a Ni-like ion.

B. Scaling of d

As was described in Sec. IV A, the variation of d versus Z or v is dominated by the variation of the shell retaining the outermost electron of ions with $q \cong \bar{q}$. Then the scaling of d would be attained if the d values are classified in terms of a mean number of electrons $\overline{n_e}=Z-\bar{q}$ instead of $\bar{q}$ as was hitherto taken by ND and Betz [see Eqs. (12) and (13)].

Figure 9 displays the d values plotted against $\overline{n_e}$ for most of existing data of ions with $Z \geq 8$. The detail at $n_e < 20$ is shown in Fig. 9(b). For $n_e < 10$, Shima *et al.*[9] already noticed the presence of the relation

$$d = 0.53 Z^{0.27} \tag{16}$$

for charge distributions of various ions whose outermost electrons are distributed in the L shell, and, in fact, Fig. 9(b) supports the relation of Eq. (16). This is the reason why the ordinate of Fig. 9 is taken to be $d/Z^{0.27}$. At the top of Fig. 9(a), the ionic shell which retains the outermost electron of ions having mean charge $\bar{q}$ is indicated. Figure 9 demonstrates that all d values can be scaled against $\overline{n_e}$ regardless of Z or v (only the envelope of many data points exhibiting the oscillatory behavior should be regarded as the scaled curve of d). The d values thus plotted oscillate against $\overline{n_e}$, where each node of the oscillation corresponds to the $\overline{n_e}$ value of closed shell or subshell of ions $1s$, $2p$, $3d$, and $4d$. It is noted that the influence of the shell structure of $4d$ core ions (or 46 electron ions) is present on d, whereas such influence was not obvious in the relation of $\bar{q}$ versus Z (Fig. 1).

The abscissa $\overline{n_e}$ corresponds to the velocity scale of ions. As is indicated in the figure for ions of F, Ar, Lu, Pb, or U, the d values for each ion species rise sharply from the limit of $\overline{n_e}=Z$ at zero velocity until they join the scaled oscillatory curve of d. For further increase of v, the d values vary along the oscillatory curve, and finally they approach the value $d=0$ at the high velocity limit or $\overline{n_e}=0$.

V. CHARGE DISTRIBUTION

A. Shell effect of charge distribution

Asymmetric charge distribution is caused due to the shell effect of $F(q)$. The boundary charge states exhibit-

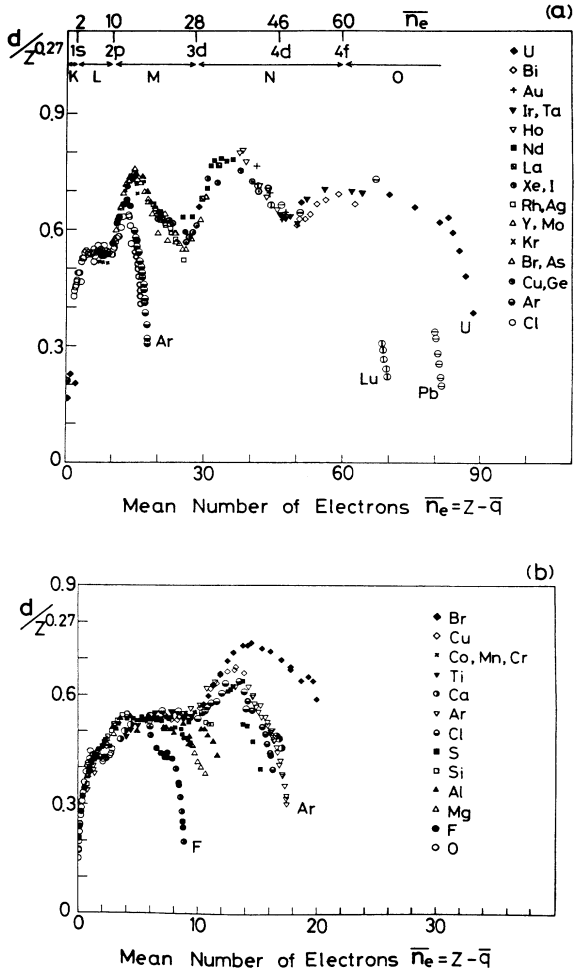

FIG. 9. Universal plot of charge distribution width d for various ions as a function of mean number of electrons attached to the ions $\overline{n_e}=Z-\bar{q}$. The details of (a) at $n_e<20$ are given in (b). K, L, M, N, or O indicates the ionic shell which retains the outermost electron of ions having mean charge $\bar{q}$ when each d value is observed in the charge distribution.

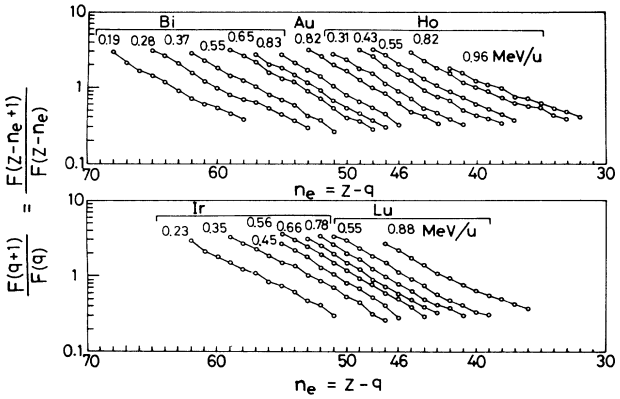

FIG. 10. Charge fraction ratio between adjacent charge states $q+1$ and q, or $Z-n_e+1$ and $Z-n_e$, where n_e stands for the number of electrons attached to ions having charge state q.

ing the shell effect are $q=Z-2$, $Z-10$, and $Z-28$. Since the enhancement of $\bar{q}$ was shown to take place around the three solid curves of $\bar{q}=Z-2$, $=Z-10$, and $=Z-28$ in Fig. 1, it can be said that the enhancement of $\bar{q}$ takes place when the shell effect of $F(q)$ appears at around the center of $F(q)$ or $q\cong\bar{q}$.

If we verify the existing data of $F(q)$ from the viewpoint of shell effect, the presence of the shell effect is more or less recognized for all the data at the above-mentioned three boundary charge states. Since it is not known if the shell effect is present at further outer shell of ions, the observed charge fraction ratio

$$F(q+1)/F(q)=F(Z-n_e+1)/F(Z-n_e)\ , \qquad (17)$$

is plotted as a function of $n_e=Z-q$ in Fig. 10. Here, n_e stands for the number of electrons attached to ions having charge state q.

Judging from the magnitudes of ionization potentials for multiply charged ions (see, e.g., the calculation by Carlson[31]), the n_e position expected for the occurrence of the shell effect at further outer shells than the $3d$ shell (Ni-like ions) is $n_e=46$ ($4d$ core ions) and $n_e=60$ ($4f$ core ions), whereas there appears little evidence of the occurrence of the shell effect in the observed values. Thus, the influence of the $4d$ shell is seen neither in $F(q)$ nor in $\bar{q}$ (see Fig. 1), but appears only in the d values (see Fig. 9).

For Ni-like ions, the occurrence of the shell effect was less significant compared with the Ne-like ions [compare Figs. 7(c) and 8(c)]. For further outer shells, this trend is more pronounced as is shown in Fig. 10. One reason for this is that, with going to outer shells, the ionization potential of ions between adjacent shells come close to each other, which destroys the shell characteristics. In addition, a relative increase of multielectron transfer or excitation compared the with single-electron transfer or excitation would contribute to the diminution of the shell effect.

B. Evaluation of $F(q)$

There exist some calculations for equilibrium charge distribution $F(q)$ of ions in carbon. For light ions ($Z\geq 10$), Zaidins[32] theoretically evaluated and presented the graphs of $F(q)$ versus v at $E<5$ MeV/u. For heavier ions, based on the existing data, Sayer evaluated an empirical formula of $F(q)$ by using skewed Gaussian distributions,[7] and Baudinet-Robinet introduced three kinds of distribution functions to be applied to $F(q)$ of ions of $9\leq Z\leq 36$ and $E<6$ MeV/u (Refs. 11–14) depending on the degree of ionization. From these references, very crude values of $F(q)$ can be estimated. As an example, $F(q)$ of 1 MeV/u Fe ions is shown in Fig. 11, where the solid curve is the calculation by Baudinet-Robinet. As is seen in the figure, observed values cannot always be reproduced by an existing empirical formula. This is because in the deduction of $F(q)$ that is basically composed of $\bar{q}$ and d the oscillation of $\bar{q}$ or d versus v or Z was not considered.

Sayer[7] and Baudinet-Robinet[14] tried to find a suitable asymmetric function of $F(q)$ that becomes important in some region of v and Z. However, the essential thing for

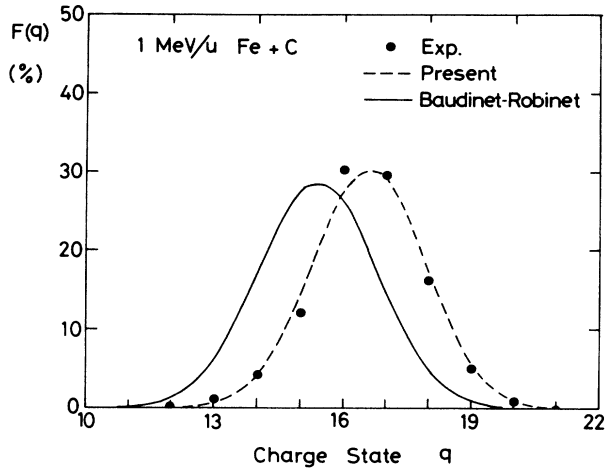

FIG. 11. Equilibrium charge distribution of 1 MeV/u Fe ions after passage through a carbon foil. Observed values by Shima *et al.* (Ref. 19), calculation by Baudinet-Robinet (Ref. 14) (solid curve), and the result of present calculation (dashed curve) are shown.

the reproducibility of actual $F(q)$ over the wide range of v and Z is the proper choice of $\bar{q}$ and d rather than the choice of distribution function. Based on this concept, improved $F(q)$ values have been evaluated in the range of $Z=4$–92 and $E=0.02$–6 MeV/u, which has been possible since precise information on $\bar{q}$ and d has become available in this paper. Our procedure is as follows.

(i) For ion species whose data are reported over the wide range of v, $\bar{q}$ values can be determined as a function of v by using the expression

$$\bar{q}=Z\left[1-\exp\left[-\sum_i (a_i v^i)\right]\right]\ , \qquad (18)$$

where a_i is the constant. For ions whose data are scarce or missing, similar expressions of $\bar{q}$ versus v are deduced by utilizing the Z oscillatory trend of $\bar{q}$ in Fig. 1 and existing data points (if any) at other velocities than those shown in Fig. 1. The $\bar{q}$ values thus obtained are listed in Table II for several combinations of Z and v.

(ii) Once the $\bar{q}$ values are evaluated, the distribution widths d are automatically determined from Fig. 9 where scaled d values are shown as a function of $\overline{n_e}=Z-\bar{q}$. The d values thus obtained are listed in Table II.

(iii) Gaussian distribution is adopted for the distribution function in which $\bar{q}$ and d values are taken from (i) and (ii), respectively. Equation (11) has been used for $F(q)$ of highly charged ions.

Results of the calculation for 1 MeV/u Fe ions are shown in Fig. 11. The degree of agreement between calculation and experiment for other Z or v is almost the same as that seen in Fig. 11 when comparable data are available. Other examples of the results for ion species $Z=9$, 25, 45, 63, and 83 are shown in Figs. 12–16 at less than 6 MeV/u. As a result of taking Z or v oscillation of $\bar{q}$ and d into account, the present calculation exhibits interesting features that (1) there arises an enhancement of the

TABLE II. Mean charges $\bar{q}$ and charge distribution widths d for several ion species and velocities obtained according to the procedure described in the text. $\bar{q}$ and d are given in units of charge.

	$Z=7$	$Z=20$	$Z=35$	$Z=50$	$Z=65$	$Z=80$
			0.02 MeV/u			
$\bar{q}$	0.942	3.07	5.22	5.59	5.66	5.56
d	0.29	1.62	1.78	2.00	2.21	2.19
			0.06 MeV/u			
$\bar{q}$	1.82	4.81	8.01	9.21	10.04	10.06
d	0.55	1.69	1.62	2.18	2.14	2.29
			0.2 MeV/u			
$\bar{q}$	3.76	8.23	12.03	16.18	17.81	19.47
d	0.85	1.44	1.60	2.22	2.00	2.35
			0.5 MeV/u			
$\bar{q}$	5.00	11.20	15.66	22.12	24.37	28.56
d	0.75	1.21	1.77	1.84	2.35	2.16
			1 MeV/u			
$\bar{q}$	5.70	12.87	19.14	25.90	29.45	33.76
d	0.69	1.21	1.93	1.70	2.51	2.17
			3 MeV/u			
$\bar{q}$	6.67	16.39	26.89	33.96	40.86	46.91
d	0.50	1.16	1.41	2.12	1.82	2.47
			6 MeV/u			
$\bar{q}$	6.96	18.57	29.90	40.65	49.75	57.68
d	0.24	0.93	1.41	1.55	2.32	2.04

envelope connecting the maxima of $F(q)$ curves, and (2) high-density $F(q)$ and low-density $F(q)$ curve groups appear alternately with the variation of v.

VI. SUMMARY

Equilibrium mean charges and charge distribution widths of ions after the passage through a carbon foil have been shown to oscillate with the variation of Z or v. Each cycle of the oscillation is in accord with the successive appearance of different ionic shells in which outermost electrons of ions are distributed. Such oscillation is observed for ions having electrons up to 46 and energies up to a few MeV/u; meanwhile for heavier and faster ions, the oscillatory behavior gradually diminishes.

It should be emphasized that the above-mentioned correlation between the shell structure of ions and $\bar{q}$ or d can be observed for ions after emergence from foil. Since charge exchange cross sections are strongly dependent on the ionization potential of ions, it is no wonder that the charge distribution of excited ions inside the foil should be influenced by the shell structure of ions. At present, such influence of the ionic shell has been observed to remain in $F(q)$, $\bar{q}$, and d of ions after the deexcitation and rearrangement of excited ions. This fact suggests that the

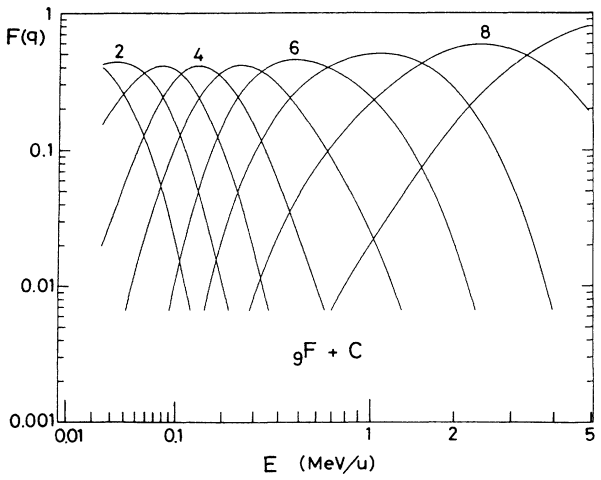

FIG. 12. Result of calculation for equilibrium charge fractions $F(q)$ of F ions after passage through a carbon foil.

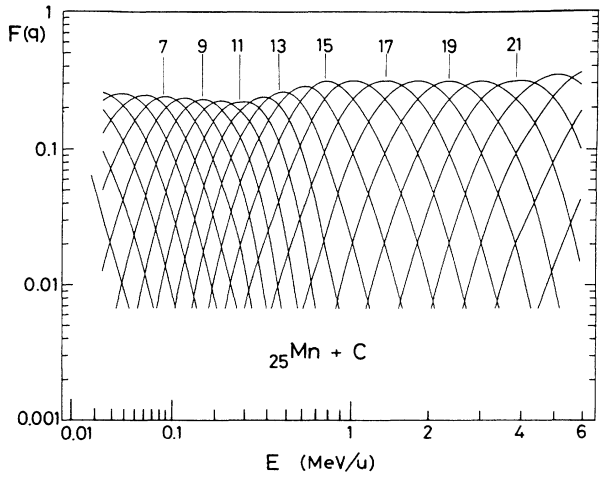

FIG. 13. Result of calculation for equilibrium charge fractions $F(q)$ of Mn ions after passage through a carbon foil.

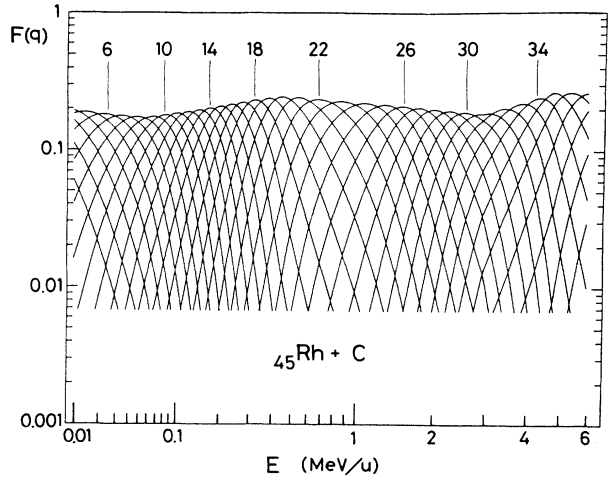

FIG. 14. Result of calculation for equilibrium charge fractions $F(q)$ of Rh ions after passage through a carbon foil.

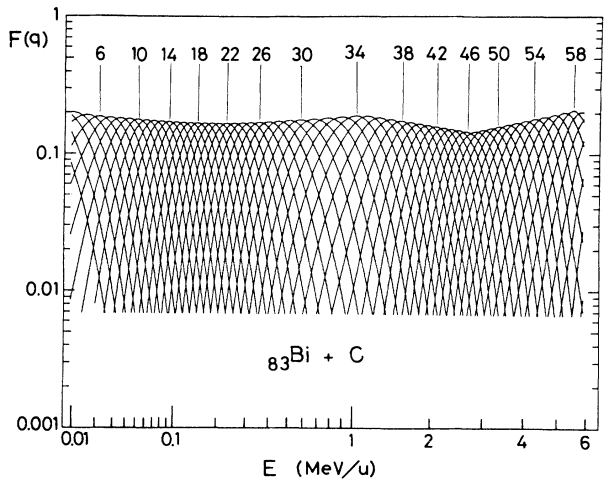

FIG. 16. Result of calculation for equilibrium charge fractions $F(q)$ of Bi ions after passage through a carbon foil.

difference of mean charges $\Delta\bar{q}$ of ions between the inside and outside of the foil caused by the post-foil Auger electron emission[1] is not so significant over the wide region of Z and v. Otherwise the phase of the oscillation of $\bar{q}$ versus Z (see Fig. 1) would not be in accord with the three curves $\bar{q}/Z = 1-2/Z$, $1-10/Z$, and $1-28/Z$, and the phase of the oscillation of d versus $\overline{n_e}$ (see Fig. 9) would have shifted from the position of the $\overline{n_e}$ value that is characterized by the shell structure of ions. In fact, Baragiola *et al.*[33] and Schneider *et al.*[34] measured the $\Delta\bar{q}$ values of Ar and other lighter ions behind carbon foils to be less than unit charge at around $v = v_0$. On the other hand, Della-Negra *et al.*[35] showed that the magnitudes of $\Delta\bar{q}$ of 1.16 MeV/u Ar ions and Kr ions in carbon foils are, respectively, zero and two in units of charges. Although the report on the measurement of $\Delta\bar{q}$ is very limited, experimental $\Delta\bar{q}$ values are at most two in units of charges, which is consistent with the above argument.

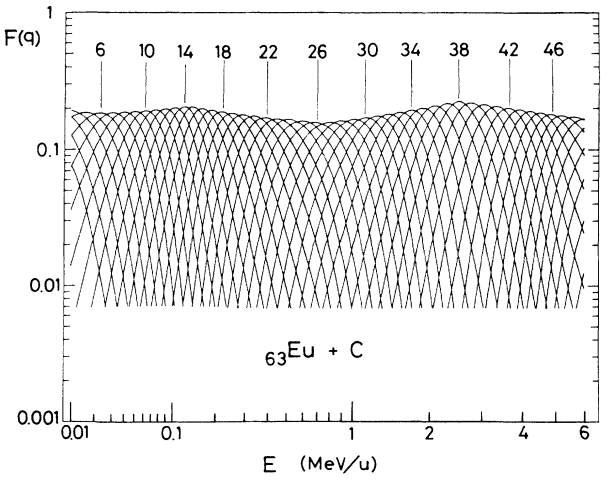

FIG. 15. Result of calculation for equilibrium charge fractions $F(q)$ of Eu ions after passage through a carbon foil.

The charge exchange process of the formation of equilibrium charge distribution is dominantly provided via the repetition of a single-electron transfer in a distant collision, where both multielectron transfer[36,37] and violent inner-shell excitation[38] as observed in a small impact-parameter collision is less likely to occur.[39] Hence, a rate equation considering one electron transfer as the dominant process can be applied to the analysis of the charge exchange process from nonequilibrium to equilibrium states as is done by many authors. Taking into account the present result that the influence of the shell effect still remains in the charge distribution of ions outside the foil, the charge exchange of the single electron belonging to the outermost shell can be considered to be mainly responsible for the formation of charge distribution, whereas tightly bound inner-shell electrons may be regarded to be a frozen core whose contribution to the final charge distribution formation is not so remarkable.

The scaling of d has first been performed based on the correlation between the shell structure of ions and d. By taking into account the Z or v oscillation of $\bar{q}$ or d, equilibrium charge distribution of ions after the passage through a carbon foil have been evaluated over the region of $Z \geq 4$ and at less than 6 MeV/u. Present evaluation of $F(q)$ would be useful considering the recent increasing demands of information on the charge distribution of ions particularly for heavier and faster ions.

ACKNOWLEDGMENTS

Authors are grateful to the crew of Tandem Accelerator Center at the University of Tsukuba and T. Kakita for their help in conducting this experiment. This work was supported in part by a Grant-in-Aid for Special Project Research on ion-beam interaction with solids from the Ministry of Education, Science, and Culture of Japan.

[1]H. D. Betz, Rev. Mod. Phys. **44**, 465 (1972).
[2]H. D. Betz, in *Applied Atomic Collision Physics*, edited by S. Datz (Academic, New York, 1984), Vol. 4, p. 1.
[3]V. S. Nikolaev and I. S. Dmitriev, Phys. Lett. A **28**, 277 (1968).
[4]K. X. To and R. Drouin, Phys. Scr. **14**, 277 (1976).
[5]K. X. To and R. Drouin, Nucl. Instrum. Methods **160**, 461 (1979).
[6]E. Baron, J. Phys. (Paris) Colloq. C1, Suppl. **40**, C1-163 (1979).
[7]O. Sayer, Rev. Phys. Appl. **12**, 1543 (1977).
[8]K. Shima, T. Ishihara, and T. Mikumo, Nucl. Instrum. Methods **200**, 605 (1982).
[9]K. Shima, T. Ishihara, and T. Mikumo, Nucl. Instrum. Methods B **2**, 222 (1984).
[10]D. Nir, S. Gershon, and A. Mann, Nucl. Instrum. Methods **155**, 183 (1978).
[11]Y. Baudinet-Robinet, H. P. Garnir, and P. D. Dumont, Phys. Lett. A **63**, 19 (1977).
[12]Y. Baudinet-Robinet, P. D. Dumont, and H. P. Garnir, J. Phys. B **11**, 1291 (1978).
[13]Y. Baudinet-Robinet, Nucl. Instrum. Methods **190**, 197 (1981).
[14]Y. Baudinet-Robinet, Phys. Rev. A **26**, 62 (1982).
[15]K. Shima, N. Kuno, T. Kakita, and M. Yamanouchi, Phys. Rev. A **39**, 4316 (1989).
[16]A. B. Wittkower and H. D. Betz, At. Data **5**, 113 (1973).
[17]K. Shima, T. Mikumo, and H. Tawara, At. Data Nucl. Data Tables **34**, 357 (1986).
[18]J. Kemmler, O. Heil, C. Biedermann, P. Koschar, M. Burkhard, H. Rothard, K. Kroneberger, K. O. Groenefeld, and W. Meckbach, Institut für Kernphysik, Johann Wolfgang Goethe-Univ., Jahresbericht, 1986 (unpublished), p. 23.
[19]K. Shima, M. Kakuta, S. Fujioka, and T. Ishihara, Nucl. Instrum. Methods B **14**, 275 (1986).
[20]J. A. Martin, Oak Ridge National Laboratory, Report No. ORNL-6420, 1988, p. 10.
[21]K. Shima, E. Nakagawa, T. Kakita, M. Yamanouchi, Y. Awaya, T. Kambara, T. Mizogawa, and Y. Kanai, Nucl. Instrum. Methods B **33**, 212 (1988).
[22]E. Baron, J. Gillet, and Ch. Ricaud, Nouv. GANIL (Grand Accelerateur National d'Ions Lourds, Caen) **26**, 32 (1988).
[23]Y. Kanai, Y. Awaya, T. Kambara, M. Kase, H. Kumagai, T. Mizogawa, and K. Shima, Nucl. Instrum. Methods A **262**, 128 (1987).
[24]K. Shima, T. Ishihara, T. Miyoshi, and T. Mikumo, Phys. Rev. A **28**, 2162 (1983).
[25]N. Bohr, Dan. Vid. Selsk. Mat.—Fys. Medd. **18**, 8 (1948).
[26]W. N. Lennard and D. Phillips, Phys. Rev. Lett. **45**, 176 (1980).
[27]W. N. Lennard, D. Phillips, and D. A. S. Walker, Nucl. Instrum. Methods **179**, 413 (1981).
[28]B. Franzke, GSI (Gesellschaft für Schwerionenforschung, Darmstadt) Report No. 83-1 (unpublished), p. 162.
[29]C. D. Moak, H. O. Lutz, L. B. Bridwell, L. C. Northcliffe, and S. Datz, Phys. Rev. Lett. **18**, 41 (1967).
[30]S. Datz, C. D. Moak, H. O. Lutz, L. C. Northcliffe, and L. B. Bridwell, At. Data **2**, 273 (1971).
[31]T. A. Carlson, C. W. Nestor, Jr., N. Wassermann, and J. D. McDowell, At. Data **2**, 63 (1970).
[32]C. Zaidins, in *Nuclear Reaction Analysis: Graphs and Tables*, edited by J. B. Marion and F. C. Young (North-Holland, Amsterdam, 1968), p. 34.
[33]R. A. Baragiola, P. Ziem, and N. Stolterfoht, J. Phys. B **9**, L447 (1975).
[34]D. Schneider, N. Stolterfoht, D. Ridder, H. C. Werner, R. J. Fortner, and D. L. Matthews, IEEE Trans. Nucl. Sci. **NS-26**, 1136 (1979).
[35]S. Della-Negra, Y. Le Beyec, B. Monart, K. Standing, and K. Wien, Phys. Rev. Lett. **58**, 17 (1987).
[36]Q. C. Kessel, Phys. Rev. A **2**, 1881 (1970).
[37]G. D. Alton, J. A. Biggerstaff, L. Bridwell, C. M. Jones, Q. Kessel, P. D. Miller, C. D. Moak, and B. Wehring, IEEE Trans. Nucl. Sci. **NS-22**, 1685 (1975).
[38]K. Taulbjerg, J. S. Briggs, and J. Vaaben, J. Phys. B **9**, 3151 (1976).
[39]C. D. Moak, IEEE Trans. Nucl. Sci. **NS-23**, 1126 (1976).